Article

Roof Strata Behavior and Support Resistance Determination for Ultra-Thick Longwall Top Coal Caving Panel: A Case Study of the Tashan Coal Mine

Jun Guo [1,2] , Guorui Feng [1,2,*], Pengfei Wang [1,2], Tingye Qi [1,2], Xiaorong Zhang [3] and Yonggan Yan [1,2]

1   College of Mining Engineering, Taiyuan University of Technology, Shanxi 030024, China; guojunfff@163.com (J.G.); wangpengfei@tyut.edu.cn (P.W.); qty198402@163.com (T.Q.); yonggantyut@163.com (Y.Y.)
2   Shanxi Province Research Center of Green Mining Engineering Technology, Shanxi 030024, China
3   Datong Coal Mine Group Company, Datong 037003, China; xiaorongzhangdt@163.com
*   Correspondence: fguorui@163.com; Tel.: +86-136-4369-7785; Fax: +86-0351-611-1086

Abstract: The Longwall Top Coal Caving (LTCC) method has greatly improved the production of ultra-thick underground coal resources. However, face fall and support closure have been becoming highly frequent accidents at the working face, and seriously threaten the safety of miners. The key to avoiding these problems is to reveal the structural evolution of the roof strata and then choose a reasonable working resistance for the hydraulic supports. According to physical modeling, theoretical analysis and field observation of the LTCC panel, four kinds of structural models can be found and defined, in consideration of the coincident movement of key strata (KS) and the mining activities of upper face in overburden strata. The KS are performed as cantilever structures, hinged structures and voussoir beam structures at three different positions in roof strata. The structural characteristics of the KS and its movement laws are shown in the four structural modes. The loads acting on the support in the four typical structural models are also analyzed. The structural instability of the broken roof strata on the upper caving panel caused by the lower ultra-thick coal seam mining is considered to be the main reason for its face's falls and support failures. Consequently, a method is proposed for calculating the working resistance of the support in the LTCC face, which is verified by the mining pressure monitoring in practice.

Keywords: Longwall Top Coal Caving; strata behavior; support resistance; igneous rock; upper gob

---

1. Introduction

Chinese coal production fell by 7.9%, and energy consumption in China grew by just 1.3% in 2016. Despite this, China remained the world's largest growth market for energy for the 16th consecutive year. The measures for reducing the capacity of the smallest, least productive mines and encouraging greater consolidation have improved the productivity and profitability of the remaining mines; at the same time, China is resuming its position as the world's largest importer of coal [1]. More efficient mining methods are encouraged in China. Longwall Top Coal Caving (LTCC) is an economical underground mining method that has been introduced and practiced in underground coal mines in China and other countries [2–4]. In China, the LTCC technology has been successfully applied to extracting ultra-thick coal seams [5–8] in which the caving height is more than 10.0 m and might even reach 20.0 m in certain coal mines [9]. However, the LTCC technology faces many challenges due to special geological conditions. The stability of the surrounding rocks [10–12] and the cavability of

top coal [13,14] in mining the ultra-thick coal seam using the LTCC method have been the focus of some researchers.

Datong coalfield is one of the largest coal production bases in China; with increasing exhaustion of the shallow resources, the deep coal seams in the Permo-Carboniferous system are becoming the main mining resources of the coalfield. As shown in Figures 1 and 2, Datong coalfield is located in Shanxi province of China, which contains four minable coal seams in the Permo-Carboniferous system. The average minable thickness of the coal seams are 3.85 m, 3.96 m, 16.8 m and 6.12 m, respectively, which provide abundant coal resources. However, the coal seams are buried in a complex geological environment caused by the intrusive igneous rock strata. As shown in Figure 2, the integrated histogram of Datong coalfield indicates that the minable S_4, 2 and 3–5 coal seams are closely buried, with average spacings of 20 m, 6 m, and 35 m, all of which are invaded by igneous rock. Additionally, the coal seams are covered by hard rock strata, including K_5 quartz sandstone, K_4 quartz sandstone and K_3 glutenite. As the largest mine of Datong coalfield, the designed annual production capacity of Tashan coal mine is 15 million tons, and the mining area is 171 km^2, including seven districts. The 3–5 coal seam has been being extracted by LTCC method in the mining area, and the designed cutting height and caving height of the face are 3.5 m and 13.0 m, respectively. A ZF10000/25/38-type four-leg hydraulic shield support (Datong, Shanxi, China) with a working resistance setting of 10,000 kN is applied to the working face. The panel width is 230 m, the dip angle is 1–3°, and the cover depth of the 3–5 coal seam is 450 m. The panel has significantly raised the production of the coal mine; however, the mining process also results in high pressure acting on the supports due to the failures of the roof strata. The commonly occurring roof failures in roadways and the crushed support accidents in the faces (shown in Figure 1) limit the efficiency and safety of the coal mine. A total of 47 hydraulic supports were crushed down during the mining of the first panel of the mine [15,16], which inflicted huge financial losses. The coal seam in Tashan Coal Mine has the following characteristics: large mining height, intrusive igneous rock, covered hard rock strata, and close upper mine out areas, which are probable factors in causing the intense dynamic accidents in the coal faces [15–18]. Simply increasing the working resistance of the hydraulic support has proved to not be a wise method for avoiding support failure in practice. Thus, it is imperative to find a reliable method for determining the working resistance in the faces of Tashan Coal Mine. Commonly, the working resistance of the support is determined by mining pressure, while the mining pressure highly depends on the broken feature and structural movement of the roof strata, which are further determined by the characteristics of the overburden strata [19]. Therefore, the interaction mechanism between hydraulic support and the roof strata should be investigated by considering the complex geological conditions of the Tashan Coal Mine.

Over the past decades, rich practical experiences have been accumulated in Chinese underground coal mining engineering; the theories of mining pressure have improved dramatically based on large amounts of field measurements, numerical modeling and physical scaled modeling studies and theoretical model studies. During the 1970s and the early 1980s, Qian and Shi [20] presented a voussoir beam mechanical model based on a large number of field measurements to derive the equilibrium conditions of the structure. Later, the theory of key strata was proposed by Qian [21], and has been widely used in controlling the behavior of the overburden strata on mining panel. Song [22] developed and perfected the theory of practical mine pressure control, which has significance in realizing coal mine safety and efficient production. In the early 2000s, Feng [23] developed a face-contacted block structure based on block theory, which promoted the basic theory of ascending mining in abandoned mining areas. Based on the above-mentioned theories, a series of studies on the interaction mechanism between hydraulic support and the roof strata has been performed. A. K. Verma and D. Deb [24,25] developed an index considering the wide variations of geomining parameters to ascertain the chock shield pressure and face convergence. They found that the mechanical parameters of the main roof and coal seam were closely related to the load on the front leg of the chock-shield support. Guo et al. [26] pointed out that the strata that can form the voussoir beam structure under normal working conditions

will break in the form of cantilever beam under hard roof conditions when defined as the key strata in the immediate roof, and the hanging length of the above-mentioned key strata was considered in determining the support working resistance. Kong et al. [12] found that the immediate roof and basic roof can form arch structures and masonry beams, respectively, after the roof collapses. Rotary collapse occurring in the upper basic roof and the static load act on the support and pillar. Ju et al. [27] proposed a calculation method for a working resistance of 7.0 m height chocks based on analyzing the structural characteristics and behavior of the key strata. Chen et al. [28] noted that the periodic weighting interval in the dip direction is equivalent to that in the strike direction, and that the strata usually form a rock-gangue arch structure in the dip direction. Wen et al. [29] applied the "strata movement and stress distribution law" and the "transferring beam" theory to build a structural mechanics model with a large mining height. They emphasized the role of the hanging roof location, thickness in achieving the greatest possible span in roof control design and support selection calculation with large mining heights. Yu et al. [30] presented a new concept and criterion for the immediate roof and main roof of the LTCC face and then developed a new analytic expression of the support working resistance based on the cantilever beam-articulated rock beam structure. Ning et al. [31] revealed the movement and fracture pattern of the double-layer hard and thick roof via microseismic monitoring to control the behavior of strata during underground LTCC panel. Huang et al. [32] proposed a method of improving the cavability of top coal in hard thick coal seams by changing the structure of the top coal and roof strata. Wang et al. [33] built a Winkler foundation beam mechanical model on the basis of the boundary support conditions of overlying high-position, hard and thick strata, and pointed out that dynamic phenomena are more easily induced when the coal mining face is under high-position hard thick strata. Huang et al. [34] put forward a method for optimizing and inverting working resistance based on the roof control effect and working resistance overrun percentage. Numerical and physical modeling studies [35,36] have also been conducted to research the roof behavior of backfill coal mining. All of the above-mentioned studies demonstrate that research into the structural characteristics and behavior of roof strata is the key to designing the support for coal faces under different geological conditions.
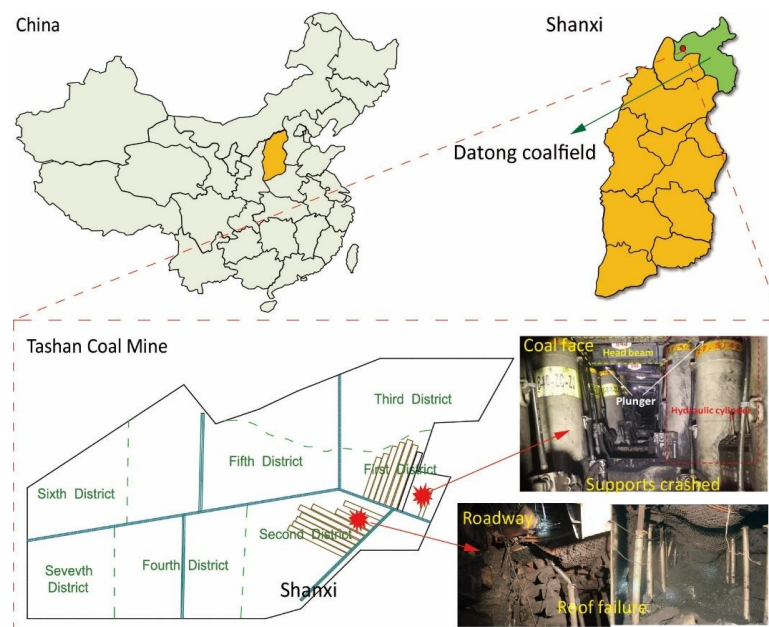

Figure 1. Location of Tashan Coal Mine.

Considering the typical geological conditions of the coal seam in Tashan Coal Mine, the roof strata behavior and support resistance determination for the ultra-thick LTCC panel have been studied. In this paper, structural evolution models of the overlying strata on the LTCC panel under an igneous

strata and upper gob were constructed based on a physical scaled model test; the evaluation of the structural evolution included the structural characteristics and mechanism analysis of the roof strata in the mining process. Then, the causes of face falls and support closure problems in the LTCC face were revealed by the analysis of the structural characteristics of the KS on the panel. Furthermore, a suitable method for selecting the working resistance for the LTCC face was proposed on the basis of a mining pressure calculation model. Finally, field measurements were used to verify the proposed structural evolution models and mining pressure behaviors of the LTCC face.
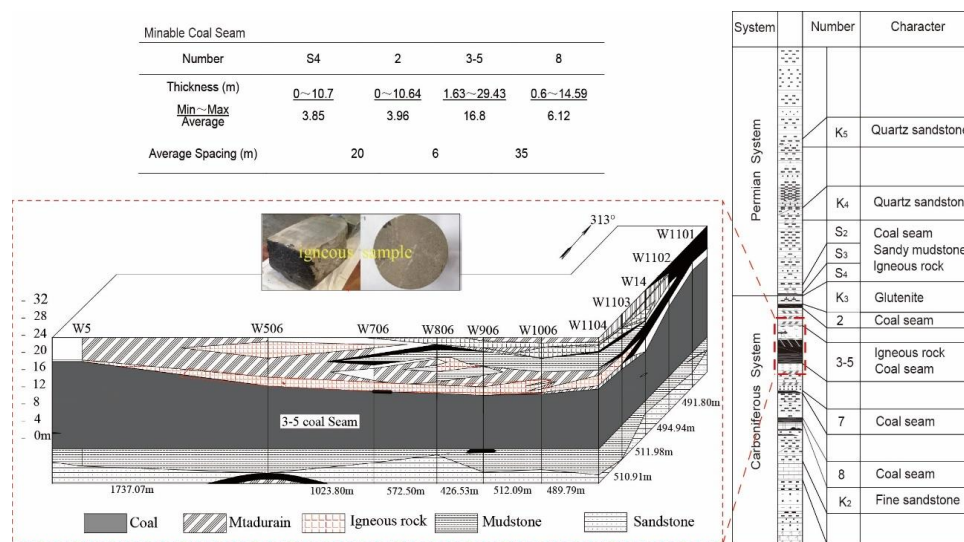

Figure 2. Geological conditions of Tashan Coal Mine.

2. Physical Modeling

Physical modeling is an effective method for simulating large-scale engineering projects, and provides researchers with information that cannot be observed and quantified in the field. Physical modeling has been applied widely in geotechnical engineering and in mining research [37,38]. To characterize the structural evolution of the strata in the overburden of the LTCC panel under an igneous sill and upper gob, a physical model was designed based on similarity theory and the rock mechanics of the strata [39]. This model revealed the structural evolution of the overlying rock strata during the extraction of the coal seam in a short test cycle.

The layered igneous sill occupies 30.5 km^2 along the top of the 3–5 Coal Seam. The distributions of the igneous sill and the mining districts of the 3–5 coal seam are shown in Figure 2. The Tashan mining area is fully covered by the igneous sill, with a thickness of 1–4.5 m, which alters the characteristic of the coal seam around it and results in favorable caving conditions for the top coal [40]. In the mining area of the first district, the average sill thickness is approximately 2.7 m. The igneous rocks are lamprophyre, which is composed primarily of dioritic porphyrite. A laboratory test [41,42] of the lamprophyre samples shows that the uniaxial compressive strength and Brazilian indirect tensile strength of the lamprophyre are 114 MPa and 8 MPa, respectively. The rock quality designation index of the lamprophyre is greater than 90% [43], indicating an extremely solid rock that can easily form a hard roof during the mining process. Furthermore, upper gobs exist in the S$_4$ coal seam, only 28 m from the super height of the 3–5 coal seam. The mining height of the S$_4$ coal seam is 3.5 m. By combining the results of the laboratory tests and field measurements with a reduction method [44–46], the physical and mechanical properties of the overlying rock strata on the mining face can be obtained, and are shown in Table 1. The position of the KS over the LTCC panel can be defined by the KS criterion [20]. In 2000, Xu [47] proposed the KS criterion, which provided a method for determining the position of the KS. The position of the KS in Tashan Coal Mine is shown in Figure 3.

Table 1. Physical and mechanical properties of overlying rock strata.

No.	Rock Strata	Unit Weight (kNm^{-3})	Elastic Modulus (GPa)	Friction Angle (°)	Cohesion (MPa)	Poisson's Ratio
1	Siltstone	23.5	18.5	37	15.2	0.24
2	Fine grained sandstone	25.6	36.0	47	24.5	0.18
3	Quartz sandstone	26.5	28.2	38	20.6	0.22
4	Silty mudstone	25.1	27.5	37	14.4	0.24
5	Medium-coarse sandstone	25.3	21.5	31	10.2	0.17
6	Glutenite	27.0	28.5	42	23.5	0.20
7	Fine sandstone	26.0	38.1	47	23.6	0.15
8	Sandy mudstone	25.9	35.1	33	8.3	0.22
9	Lamprophyre	27.4	60.9	52	24.8	0.12
10	Coal	14.3	8.4	28	14.3	0.32

Thickness	Histogram	Lithologic			Remarks
35.73 m		Siltstone			KS2
13.64 m		Fine grained sandstone			
20.50 m		Quartz sandstone			
12.30 m		Silty mudstone			Upper Goaf Area
8.41 m		Medium-coarse sandstone			
3.85 m		S4 Coal seam			KS2
15.11m		Glutenite			
3.90 m		Silty mudstone			
1.99 m		2 Coal seam			KS1
2.58 m		Fine sandstone			CavingHeight
3.70 m		Sandy mudstone			
2.66 m		Lamprophyre			Cutting Height
16.80m		3-5 Coal seam			

Figure 3. Stratigraphic column of the coal face.

In this paper, four similarity coefficients (C_L, C_σ, C_γ and C_t) are defined for the geometry, stress, unit weight and time, respectively, to satisfy the following similarity criteria:

$$\begin{cases} C_L = L_H/L_M \\ C_\gamma = \gamma_H/\gamma_M \\ C_\sigma = C_L \times C_\gamma \\ C_t = \sqrt{C_L} \end{cases} \tag{1}$$

In this study, the geometric scale coefficient (C_L) is selected to be 150, taking into consideration the limited space of the test platform and the restricted simulation range of 3 m (width) × 3 m (height) × 0.2 m (depth). The materials used in this experiment were plaster, precipitated calcium carbonate, sand, and cement. Each rock stratum in the physical model is manufactured using similar materials with varying mixture proportions to satisfy the similarity constant for density C_γ of 1.7 and is mutually separated by mica powder that is homogeneously spread on the rock surfaces.

In this experiment, the rock strata is simulated only at depths from 180 m to 480 m, and the weight of the inaccessible strata above 180 m is simulated with a pressurized water container, with its pressure being controlled by a pressure regulator to satisfy the overburden pressure. The additional pressure q_a can be determined by Equation (2). The final physical model in this paper is shown in Figure 4.

$$\begin{cases} q_a = \dfrac{\gamma h}{C_L \cdot C_\gamma} \\ \gamma = \rho g \end{cases} \tag{2}$$

where ρ is 2500 kg/m^3; g is 9.8 N/kg; and h is the height of the inaccessible strata greater than 180 m.
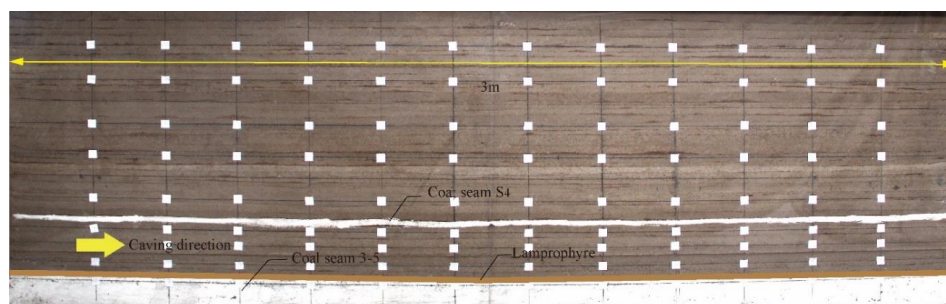
Figure 4. Physical model.

3. Modeling Results

In the experiment, the upper S_4 coal seam is first removed from the model to simulate its mining process. The model was allowed to rest for three days until the surrounding rock of the S_4 coal seam had fully caved and the model had regained its stress equilibrium. Next, the 3-5 coal seam was removed to simulate its extraction. The structural characteristics of the strata on the upper gob in the S_4 coal seam and the structural evolution process of the overburden strata on the LTCC panel are described in the following sections.

3.1. Structural Characteristics of the Strata on the Upper Gob

As shown in Figure 5a, three zones are formed in the overburden strata on the upper gob of the S_4 coal seam. The three zones are the caved zone, fractured zone and continuous deformation zone. Based on the direct measurements from the model, the heights of the caved and fractured zones are 0.08 m and 0.16 m, respectively. Figure 5a shows that the roof caving angle of the upper gob reaches 55°, where the roof caving angle is a parameter used to describe the characteristic of the overburden strata on the gob area. The roof caving angle is defined as the angle between the fractured surface and the bedding surface of the roof strata. Three days after removing the S_4 coal seam, a compacting area is formed in the middle of the gob area, which is shown in Figure 5b.
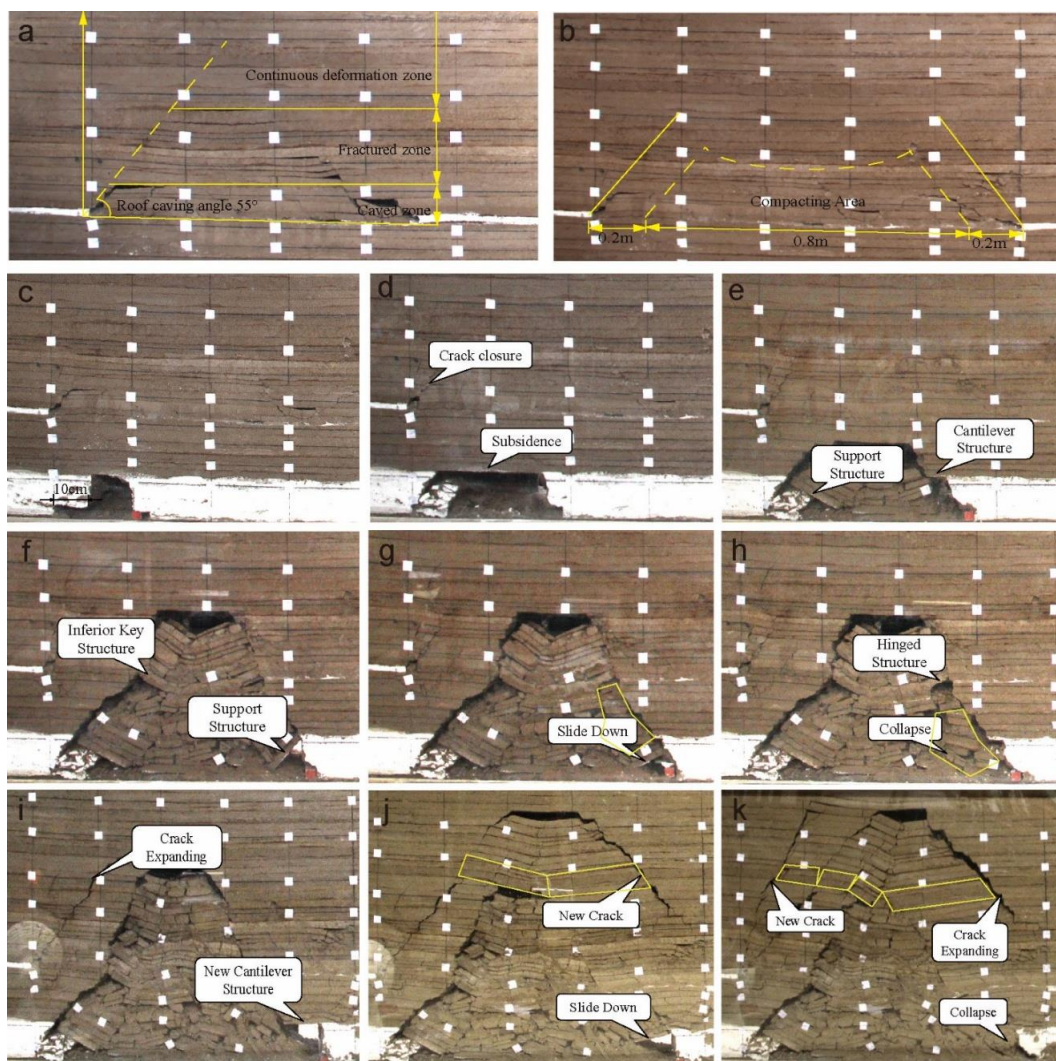

Figure 5. Roof strata behavior of the LTCC panel under an igneous sill and upper gob.

3.2. Structural Evolution of the Strata on the LTCC Panel

According to the coal mine safety regulations [48], it is not allowed to exploit the top coal (about 15 m long) in the initial mining stage; thus, 0.1 m top coal is retained in the physical model, which is shown in Figure 5c. Figure 5d shows that the advancement of the coalface improves the subsidence of the immediate roof and leads to the closure of the crack near the coal wall of the upper gob. As is shown in Figure 5e, when the coalface advances to 0.55 m (corresponding to 82 m in practice), the roof strata suddenly caved, and the broken lamprophyre strata develops into a support structure and then a cantilever structure, in turn. The maximum caving height reaches 0.25 m (corresponding to 37.5 m in practice) at this stage. When the working face advances 0.69 m (corresponding to 103.5 m in practice), the cantilever structure is fractured at its limit length of 0.08 m (corresponding to 12 m in practice) and then develops into a support structure, and the two sides of the support structure contact with the top coal and the gangue in the gob area. Additionally, periodic breaks occur in the overburden strata, and the maximum caving height increases to 0.42 m (corresponding to 63 m in practice); the structural features of the overburden strata at this stage are shown in Figure 5f. In the top coal caving process, as shown in Figure 5g, a part of the strata moves down with the sliding of the support structure. The further advancement of the face promotes the sliding of the support structure, and a hinged structure is formed at a higher level of the overlying strata, as shown in Figure 5h, which limits the subsidence of the upper caved strata. Cantilever structures and hinged structures are periodically formed in the overburden strata with the advancement of the face; meanwhile, the increased caving distance leads to an expanding range of fracture zone. Figure 5i shows that the closed crack in Figure 5d is expanding, and a new cantilever structure is formed in the lamprophyre strata. As shown in Figure 5j, the sliding of the support structure induces a new crack, which originates from the boundary of the upper gob. Meanwhile, the higher-level strata break down at a vertical distance of 0.93 m (corresponding to 139.5 m in practice) from the coal seam and form a hinged structure. When the lower support structure in Figure 5k collapses to the gob area, a new crack expands along the other boundary of the upper gob; simultaneously, the hinged structure develops into a voussoir beam structure.

4. Discussion

The physical modeling results have shown the typical structures of the roof strata developed in the caving process. In order to describe the behaviors of the roof strata more visually, we have summarized four typical structural models of the LTCC panel in Tashan Coal Mine. Additionally, mechanical analysis of the cantilever structure and voussior beam structure have also been investigated in order to describe to characteristics of the structures, which provides a foundation for the determination of the support resistance for the ultra-thick Longwall Top Coal Caving panel.

4.1. Structural Models of Roof Strata

In the context of the theory of KS [21], the strata that control the activities of all or a portion of the rock mass are called the KS. Based on the results of the scaled model, it can be concluded that there are three KS (lower KS1, middle KS2 and upper KS3) for extracting the ultra-thick seam. The different structures of the KS result in different strata behaviors. Additionally, the broken features of the overlying strata are indirectly influenced by the crack caused by the upper gob. In consideration of the influence of the KS and upper gob, four structural models are established for the LTCC extraction, and the models are described in Figure 6.

(1) Model A represents the formation of a cantilever structure in the lower KS. It is characterized by an igneous sill above the coal seam, and part of the roof strata on the working face is controlled by KS1.

(2) Model B demonstrates the formation of a support structure in the lower KS and a hinged structure in the middle KS. In this model, the support structure develops from the cantilever structure in

model A, and the hinged structure develops from the middle KS2. The movement of the strata between KS1 and KS2 is controlled by the support structure and KS2.

(3)   Model C represents the influence between the adjacent KS. In this model, the support structure in KS1 slides down, while the hinged structure in KS2 collapses under the pressure of the broken block in KS3. The behavior of the overlying strata is controlled by the movement of KS1 and KS2.

(4)   Model D describes a voussoir beam structure formed in the upper KS3. In this model, a large part of the strata between KS2 and KS3 topple down and break in advance of KS1 and KS2, which are impacted by the break of KS3 and the expanding crack in the upper gob. The strata behavior is controlled by KS3.
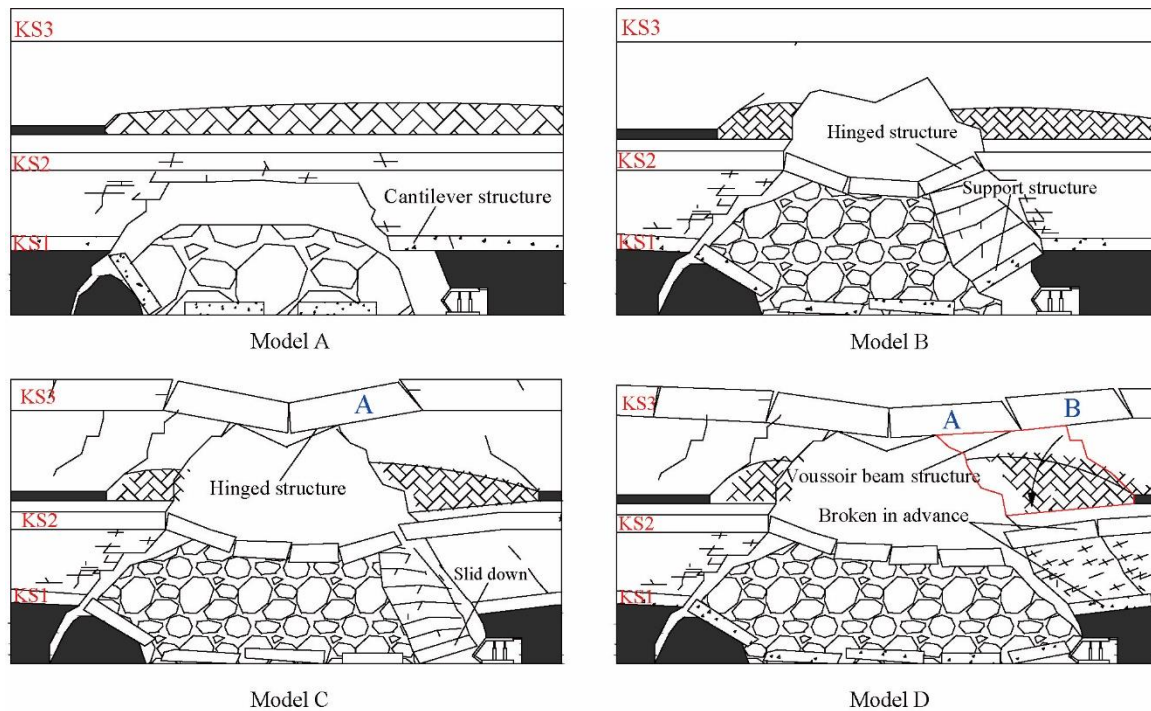
Figure 6. Structural models of the overlying strata on the LTCC panel. (Blue part A and B refer to the two key blocks in voussoir beam structure of the key roof strata.).

4.2. Structural Characteristics of KS

Based on the results of the scale model and the structural models of the overlying strata on the LTCC panel, it can be observed that the lower KS1 mainly develops into a cantilever and support structure, while the middle KS2 forms a hinged structure under certain conditions, and the upper KS3 mainly develops into a voussoir beam structure. The behaviors of the KS affect the structural evolution of the overlying strata and determine the mining pressure. The mechanical behaviors of the structures are analyzed in the next section.

KS1 develops into either a cantilever structure or a support structure in the advancement of the working face.

(1)   Cantilever structure

The mechanical analysis of a cantilever structure in the lamprophyre strata is shown in Figure 7, and the torque equilibrium equation is shown as follows:
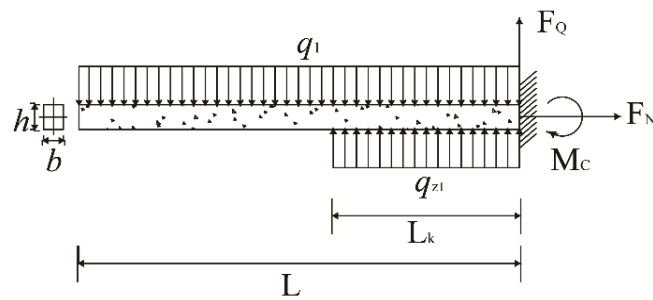
Figure 7. Cantilever structure of KS1.

$$M_C = \frac{1}{2} \cdot q_1 \cdot L^2 - \frac{1}{2} q_{z1} \cdot L_k{}^2 \tag{3}$$

where q_1 is the overlying vertical load on the cantilever structure, the L is the limited span of the cantilever, q_{z1} is the vertical support load from the top coal and L_k is the face-to-gob distance.

The overlying vertical load on the cantilever structure is defined as follows:

$$q_1 = \sum_{i=1}^{n} h_i \cdot \gamma_i \tag{4}$$

where h_i is the thickness of the overlying strata (m) and γ_i is the density of overlying strata (N/m^3).

The vertical support load on the cantilever structure that from the top coal is defined as follows:

$$q_{z1} = \frac{P}{B \cdot L_K} \tag{5}$$

where P is the support resistance (N) and B is the width of the hydraulic support (m).

The ultimate strength of the cantilever is defined as follows:

$$[\sigma] = \frac{6M_c}{bh^3} \tag{6}$$

where M_c is defined by Equation (3), b and h are the width and height, respectively, of the section of the cantilever beam.

Based on these equations, the limited span of the cantilever can be derived as follows:

$$L = \sqrt{\frac{[\sigma]b \cdot h^2 + 3\frac{P}{B}L_k}{3\sum h_i \cdot \gamma_i}} \tag{7}$$

(2) Support structure

The mechanical analysis of a support structure in the lamprophyre strata is shown in Figure 8, and the force equilibrium equation in this structure is defined as follows:
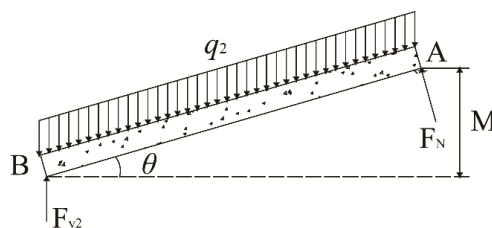

Figure 8. Support structure of KS1.

$$F_N = \frac{q_2 L}{2} \cos \theta \tag{8}$$

where F_N is the support force from the top coal, q_2 is the overlying vertical load on the cantilever ($q_2 = \sum h_{2i} \cdot \gamma_{2i}$, the h_{2i} and γ_{2i} are the thickness and the unit weight of the rock strata that controlled by the cantilever structure in caved zone) and θ is the rotating angle of the cantilever ($\theta = \arcsin M/L$) in this state.

Before the fracture of upper KS3, the middle KS2 formed a hinged structure. The stability of the structure is determined by the maximum rotation $\Delta_{\max}$ and allowed rotation Δ of the hinged block. If $\Delta_{\max} \leq \Delta$, KS2 can form a hinged structure. Figure 9 shows the rotation of KS2. The allowable rotation of the hinged block can be expressed as:
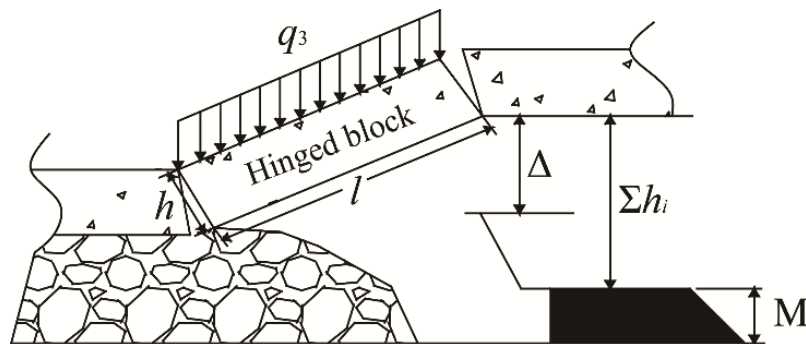

Figure 9. Hinged structure of KS2.

$$\Delta = M(1 - p_1) + (1 - K_p) \sum h_i \tag{9}$$

where Δ is the allowable rotation of the hinged block, M is the height of the coal seam, K_p is the bulking factor of the immediate roof, Σh_i is the thickness of the immediate roof under KS2, and p_1 is the mining-ratio of the coal seam. The maximum rotation [30] of the hinged block can be expressed as:

$$\Delta_{\max} = h - \frac{q_3 l^2}{kh[\sigma_c]} \tag{10}$$

where $\Delta_{\max}$ is the maximum rotation of the hinged block, h is the height of KS2, q_3 is the load on KS2, l is the broken length of KS2, $k = 0.1h$, $[\sigma_c] = 0.30.35R_c$, and R_c is the compressive strength of KS2 as measured in the laboratory.

In structural model D of the overlying strata on the LTCC panel, KS3 develops into a voussoir beam structure, and the broken block B plays an important role in maintaining stability of the structure. The mechanical analysis for block B is shown in Figure 10. Basically, the key block has two modes of the instability, namely the instability due to the sliding (S) and the rotation (R). The major factors that affect the stability of the structure are rotational angle of the voussoir beam, ratio of length and height, the rock type and the height of carrying rock strata [49]. These factors are considered to establish the "S-R" stability criterion. This criterion can be used for quantitative analysis of effect of overlying strata above the working face [20].
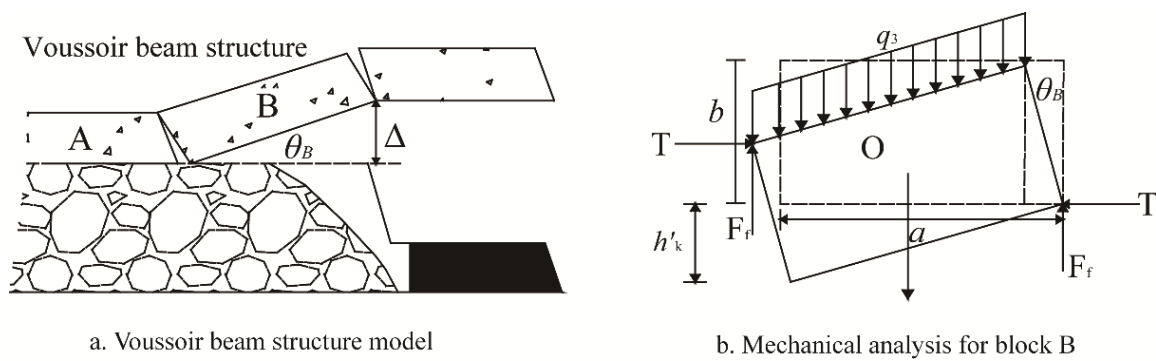
a. Voussoir beam structure model　　　　b. Mechanical analysis for block B

Figure 10. Voussoir structure and mechanical analysis for block B.

On the basis of the 'S-R' stability criterion [47], the stability of a voussoir beam structure is determined by the following equation:

$$\begin{cases} h + h_1 \le \frac{\sigma_c}{30\rho g}\left(\tan\varphi + \frac{3}{4}\tan\,\sin\theta_B\right)^2 \\ h + h_1 \le \frac{0.15\sigma_c}{\rho g}\left(i^2 - \frac{3}{2}i\sin\theta_B + \frac{1}{2}\sin^2\theta_B\right) \end{cases} \tag{11}$$

where $h + h_1$ is the total thickness of the loading and bearing layers of the structure, σ_c is the compressive strength of the bearing layer, ρg is the specific weight of the bearing layer, φ is the friction angle between the blocks, i is the size of the caving block ($i = b/a$, where a is the length of the block, and b is the thickness of the caving block), and θ_B is the rotating angle of block B in this state (with $\theta_B = \Delta/a$).

As mentioned above, analysis of the characteristics of KS indicates that many factors affect the structural feature and stability of KS. These factors can be divided into two basic aspects: internal factors and external factors. The internal factors include the physical and mechanical properties of the overlying strata, while the external factors mainly include the caving height of the coal seam and the failure of surrounding rock that caused by an adjacent coal seam. Thus, the super-high caving face, the layered igneous sill, and the upper gob play an important role in producing abnormal mining pressure in the LTCC face of the Tashan Coal Mine.

4.3. Support Resistance Determination

The previous analysis indicates that there are four typical types of structural model on the advancing LTCC face. To choose a reasonable working resistance, the load on the supports in the different models must be known. The maximum load calculated by the models can be used to design the working resistance of the hydraulic supports in the face and further provide appropriate roof management technique during field operations.

In the caving process of the immediate roof, a cantilever structure is formed in KS1. The strata in the fractured zone can bear the load of the upper strata; thus, the load on the supports is primarily determined by the weight of the top coal, cantilever structure and immediate roof in the caved zone. The model for the mining pressure calculation is described in Figure 11a. Thus, the equation for calculating the load can be expressed as:

$$\begin{cases} P_1 = Q_1 + Blh_1\gamma_1 + Q_t \\ Q_1 = Bl\Sigma h_{i1}\gamma_{i1} \\ Q_t = Bl_k h_t \gamma_t \end{cases} \tag{12}$$

where P_1 is the load on the supports in model A, Q_1 is the weight of the immediate roof that controlled by the cantilever structure in the caved zone, Q_t is the weight of the top coal seam that controlled by the

cantilever structure in the caved zone, B is the width of hydraulic support (m), l is the broken length of the cantilever structure (m), l_k is the face width of the hydraulic support (m), h_t is the thickness of top coal seam (m), γ_t is the unit weight of the top coal seam (N/m^3), $\sum h_{i1}$ is the thickness of the immediate roof in the caved zone (m), and γ_{i1} is the average unit weight of the immediate roof in the caved zone (N/m^3).

　　When the cantilever structure in KS1 develops into a support structure, as is shown in model B, the broken blocks of KS2 form a hinged structure. The model for the load calculation is shown in Figure 11b. The load should be calculated using three parts: the first part is the weight of the rock in the caved zone (Q_2), the second part is the weight of the top coal (Q_t), which can be calculated according to the roof control distance of the hydraulic supports, and the third part is the force needed to maintain a stable support structure (P_{H2}). The weight of the rock in the caved zone is determined by the self weight of KS1 and the strata weight between KS1 and KS2. Thus, the equation for calculating the load can be expressed as:

$$\begin{cases} P_2 = Q_2 + Q_t + P_{H2} \cdot \cos\theta \\ Q_2 = Bl_2 \Sigma h_{i2} \gamma_{i2} + Bl_2 h_1 \gamma_1 \end{cases} \tag{13}$$

where P_2 is the load on the supports in model B, l_2 is the broken length of KS1 (m), $\sum h_{i2}$ is the thickness of the immediate roof between KS1 and KS2 (m), γ_{i2} is the average unit weight of the immediate roof between KS1 and KS2 (N/m^3), θ is the support angle of the support structure (°), and P_{H2} can be calculated using Equation (8).
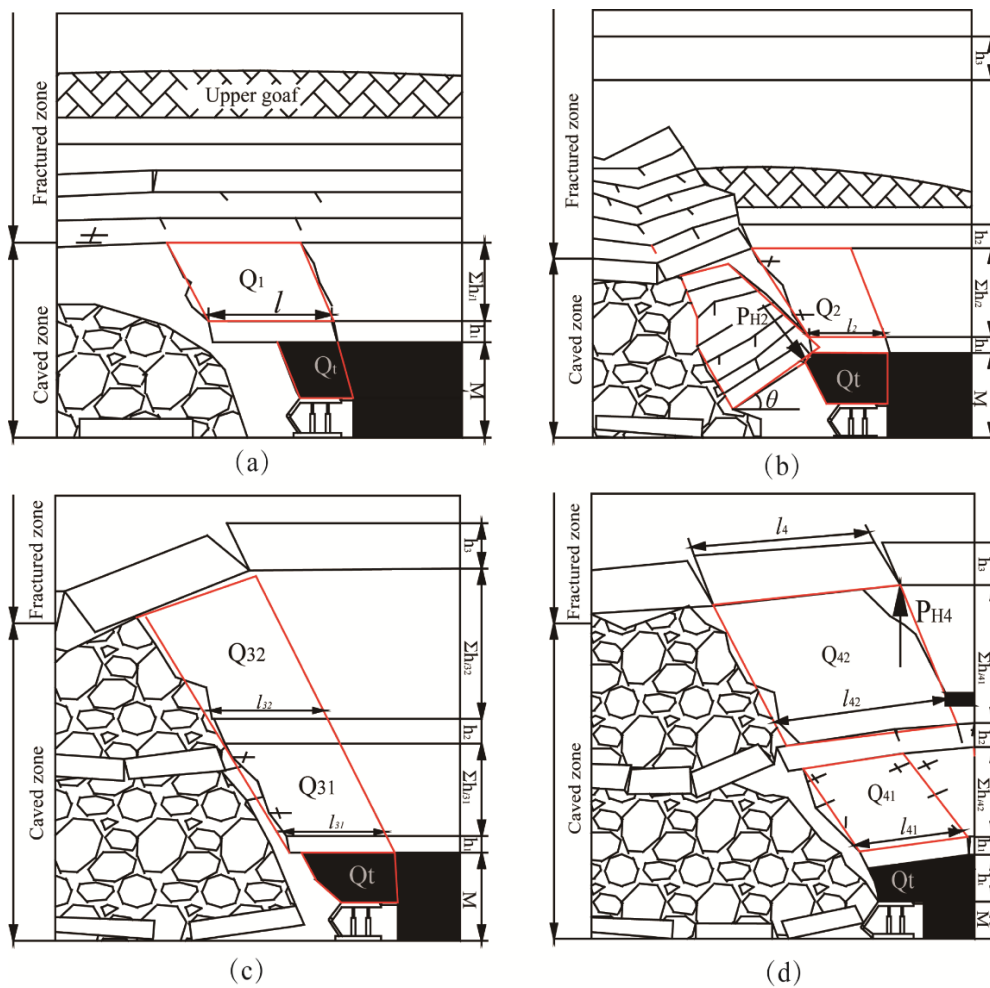

Figure 11. Support resistance calculation models.

The sliding of the support structure increases the rotating space for KS2, which, combined with the load from the broken block in KS3, causes the hinged structure in KS2 to collapse into the gob area; simultaneously, the broken blocks of KS3 develop into a new hinged structure. The model for the working resistance calculation is described in Figure 11c. The hinged structure can transfer its own weight and the load of the upper strata to the gob area and the advancing area of the working face. Therefore, the load is calculated using two parts: one part is the weight of the top coal (Q_t) and the other part is the weight of the rock in the caved zone (Q_3), which is determined by the load from the weight of KS1, KS2 and the strata between the three KS in caved zone. Thus, the equation for calculation of load can be expressed as:

$$\begin{cases} P_3 = Q_3 + Q_t \\ Q_3 = B(h_1\gamma_1 l_{31} + h_2\gamma_2 l_{32}) + Q_{31} + Q_{32} \\ Q_{31} = Bl_{31}\Sigma h_{i31}\gamma_{31} \\ Q_{32} = Bl_{32}\Sigma h_{i32}\gamma_{32} \end{cases} \tag{14}$$

where P_3 is the load on the supports in model C, γ_{31} is the unit weight of the immediate roof between KS1 and KS2 (N/m^3), γ_{32} is the unit weight of the immediate roof between KS2 and KS3 (N/m^3), $\sum h_{i31}$ is the thickness of the rocks between KS1 and KS2 (m), and $\sum h_{i32}$ is the thickness of the rocks between KS2 and KS3 (m).

When the crack that originated from the boundary of the upper gob expands to KS3, a large part of the rock mass between KS2 and KS3 rotates into the gob area; simultaneously, KS3 develops into a voussoir beam structure. The model for the working resistance calculation is described in Figure 11d. In this model, the load can be calculated using three parts: the weight of the top coal (Q_t), the weight of the rocks between the three KS and the self weight of KS1 and KS2 (Q_4), and the load that balances the hinged block in the voussoir beam structure of KS3 (P_{H4}), which can be calculated according to the theoretical equation derived from the voussoir beam structure. Thus, the equation for the load calculation of model D can be expressed as:

$$\begin{cases} P_4 = Q_4 + Q_t + P_{H4} \\ Q_4 = B(h_1\gamma_1 l_{41} + h_2\gamma_2 l_{42}) + Q_{41} + Q_{42} \\ Q_{41} = Bl_{41}\Sigma h_{i41}\gamma_{41} \\ Q_{42} = Bl_{42}\Sigma h_{i42}\gamma_{42} \\ P_{H4} = [2 - l_4 \cdot \tan(\varphi - \alpha)/2(h_3 - \delta_3)]Q_{43}B \end{cases} \tag{15}$$

where P_4 is the load on the supports in model D, γ_{41} is the unit weight of the immediate roof between KS1 and KS2 (N/m^3), γ_{42} is the unit weight of the immediate roof between KS2 and KS3 (N/m^3), $\sum h_{i41}$ is the thickness of the rocks between KS1 and KS2 (m), $\sum h_{i42}$ is the thickness of the rocks between KS2 and KS3 (m), l_{41} is the breaking length of KS1, l_{42} is the breaking length of KS2, l_4 is the breaking length of KS, h_3 is the thickness of KS3, φ and α are the friction angle between the rock blocks and the broken angle of the rock block, respectively, δ_3 is the subsidence of the broken block (m), and Q_{43} is the total weight of the broken block of KS3 and its controlled overlying strata (N/m).

In conclusion, these four models indicate that the KS plays an important role in controlling the movement of the overlying strata. Based on the four structural models, the loads for the four typical regions are calculated in Table 2. Consequently, the load is relatively low during the initial coalfield exploitation when the overburden strata are controlled by the structures in KS1 and KS2. The load obviously increases when the lower LTCC face is advancing to the boundary of the upper gob, and the maximum load reaches 14,850 kN.

Table 2. The load on hydraulic support calculated by mathematical equation.

Structural Model	Model A	Model B	Model C	Model D
Load (kN)	2570	6250	12,150	14,850

5. Field Mining Pressure

The field practice indicates that thirty-five columns of the hydraulic supports were crushed by the irregular mining pressure when one of the working faces advanced form 90 m to 160 m. Field mining pressure monitoring had been conducted in Tashan Coal Mine. The field measurement diagram is shown in Figure 12.

Two typical mining pressure curves in Figure 13a,b show that the loads on the columns reach and even go beyond their ultimate state. In order to verify the load calculated by the proposed method, the practical maximum pressure on the support is shown in Figure 13c. The green dashed line shown in Figure 13c represents the working resistance of the hydraulic supports applied in the LTCC face. The maximum pressure on the support is cyclically increased with the increase in the face advancing distance, which is caused by the periodic breakage and incremental caving height of the overburden strata. The curve of the maximum pressure in Figure 13c can be divided into four cycles, and the maximum values of the load in the four cycles are 2600, 6860, 11,600 and 14,270 kN, respectively. Obviously, the practice results are basically in accordance with the mathematical results, but the maximum load calculated by the proposed method is just higher than the practical value. Field practice also confirms that the ZF15000/28/52 hydraulic support (Datong, Shanxi, China) has been applied to the present panels in the Tashan Coal Mine, and its working resistance improved to 15,000 kN.
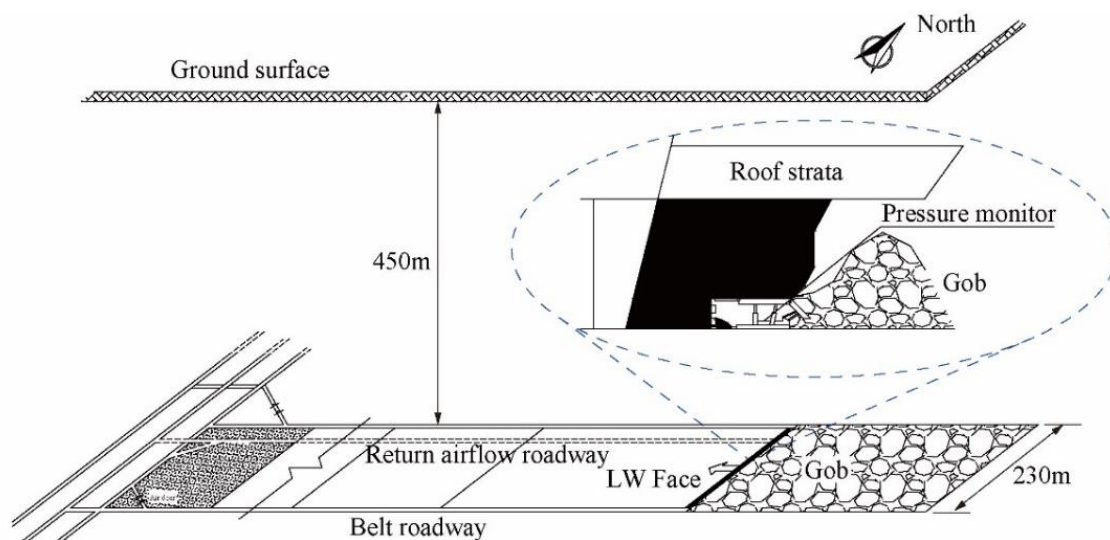
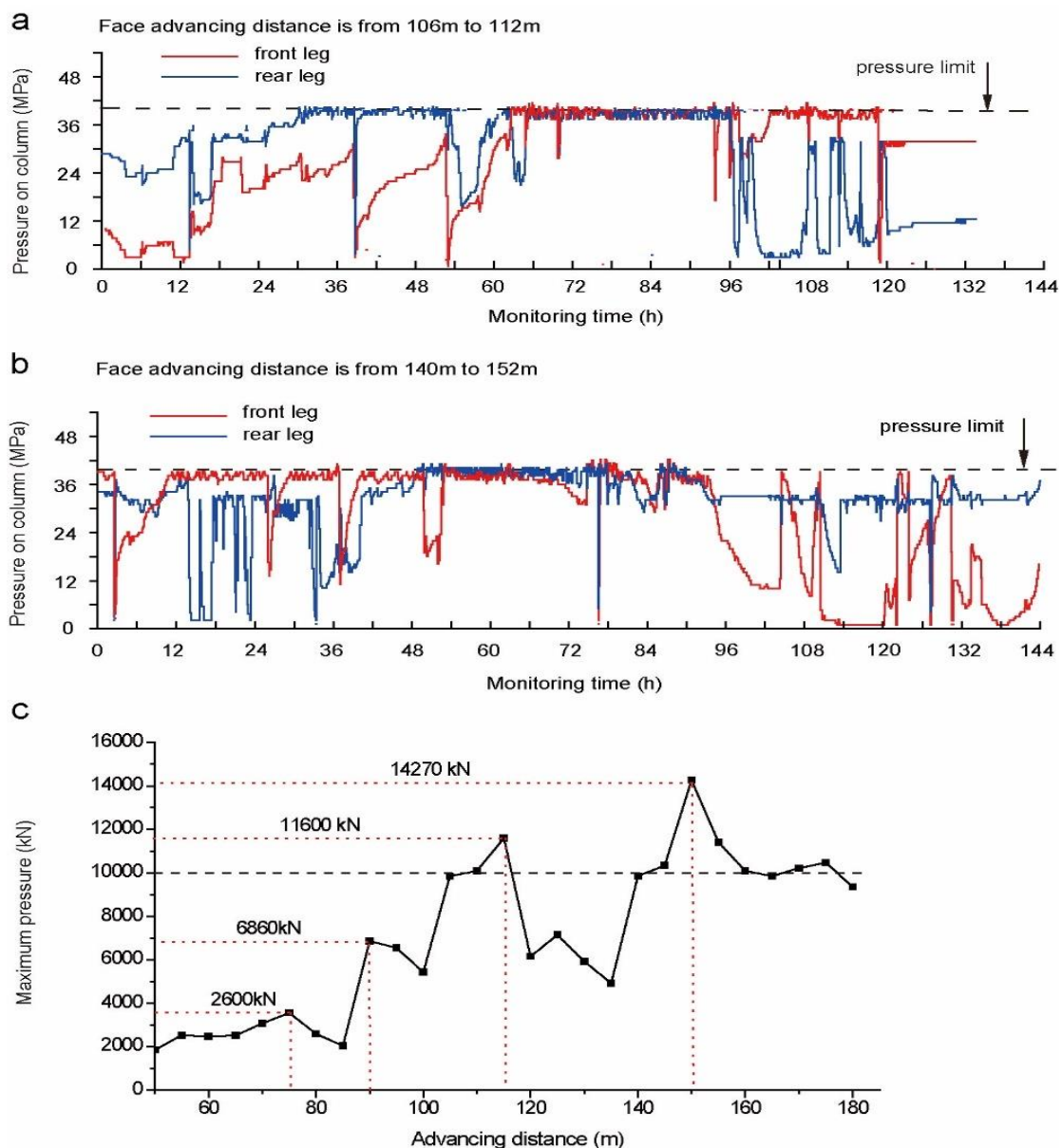**Figure 12.** Field measurement diagram in Tashan Coal Mine.

Figure 13. Typical mining pressure on the columns and maximum load on support. ((**a**). Mining pressure on column when face advancing from 106 m to 112 m; (**b**). Mining pressure on column when face advancing from 140 m to 152 m; (**c**). Practical maximum pressure on the support in mining process).

6. Conclusions

The structural evolution of the roof strata on the LTCC panel under an igneous sill and upper gob in the Tashan Coal Mine in China is different from that of a normal LTCC panel. Three KS control the movement of the overburden strata and determine the mining pressure in the LTCC panel: KS1 is developed from the igneous sill, KS2 is located between the ultra-thick coal seam and upper gob, and KS3 is in the main roof of the overburden strata. The cracks caused by the extraction of the upper coal seam affect the movement of the KS and further increase the mining pressure on the support in the lower LTCC panel.

Four typical structural evolution models of the overburden strata are constructed based on the physical scale model study. KS1 develops into a cantilever structure in the initial caving process of the immediate roof strata, which is shown in model A. Model B mainly represents the support structure in

the lower KS1 and the hinged structure in the middle KS2. In model C, the broken blocks in KS3 are hinged together and form a hinged structure. Model D demonstrates an advancing fracture in KS1 and KS2, and a voussoir beam structure in KS3. The expanding crack that originates from the boundary of the upper gob promotes rotation of the large portion of rock mass between KS2 and KS3 in mode D, which increases the load on the LTCC panel and induces face falls and support closure. The structure evolution models reveal the reason for accidents in the LTCC panels and provide some suggestions for other coal mines in the similar geological conditions.

Taking the structural evolution of the roof strata and strata behaviors of the KS into consideration, a method is proposed for calculating the working resistance of the hydraulic support in the LTCC panel that are influenced by an igneous sill and upper gob. The value calculated by model D is selected to determine the suitable working resistance for the support in the face. The working resistance for the hydraulic supports of the face in Tashan Coal Mine is determined to be 14,850 kN, which is generally in accordance with the results of the monitoring data in practice. Thus, the proposed method is applicable to determine the working resistance of the supports in the other unexploited mining districts of the Tashan Coal Mine. This case study aimed to study the roof strata movement patterns under the specific conditions of an ultra-thick coal seam with a hard roof, which could be used to deal with the problems of the Tashan Coal Mine directly and have important guiding significance for other coal mines in extracting the coal seams in the Permo-Carboniferous system of China and are also helpful for mining the ultra-thick coal seams under hard roof strata.

Author Contributions: Jun Guo and Guorui Feng conceived and designed the experiments; Jun Guo and Yonggan Yan performed the experiments; Xiaorong Zhang collected the practical data; Jun Guo and Pengfei Wang analyzed the data; Tingye Qi contributed materials and analysis tools; Jun Guo wrote the paper.

Conflicts of Interest: The authors declare no conflict of interest.

References

1. BP. *BP Energy Outlook Energy 2017*; BP: London, UK, 2017.
2. Vakili, A.; Hebblewhite, B.K. A new cavability assessment criterion for Longwall Top Coal Caving. *Int. J. Rock Mech. Min. Sci.* **2010**, *47*, 1317–1329. [CrossRef]
3. Alehossein, H.; Poulsen, B.A. Stress analysis of longwall top coal caving. *Int. J. Rock Mech. Min. Sci.* **2010**, *47*, 30–41. [CrossRef]
4. Khanal, M.; Adhikary, D.; Balusu, R. Prefeasibility study—Geotechnical studies for introducing longwall top coal caving in Indian mines. *J. Min. Sci.* **2014**, *50*, 719–732. [CrossRef]
5. Yu, B.; Zhao, J.; Xiao, H. Case Study on Overburden Fracturing during Longwall Top Coal Caving Using Microseismic Monitoring. *Rock Mech. Rock Eng.* **2017**, *50*, 507–511. [CrossRef]
6. Si, G.; Shi, J.Q.; Durucan, S.; Korre, A.; Lazar, J.; Jamnikar, S.; Zavšek, S. Monitoring and modelling of gas dynamics in multi-level longwall top coal caving of ultra-thick coal seams, Part II: Numerical modelling. *Int. J. Coal Geol.* **2015**, *144–145*, 58–70. [CrossRef]
7. Si, G.; Jamnikar, S.; Lazar, J.; Shi, J.Q.; Durucan, S.; Korre, A.; Zavšek, S. Monitoring and modelling of gas dynamics in multi-level longwall top coal caving of ultra-thick coal seams, part I: Borehole measurements and a conceptual model for gas emission zones. *Int. J. Coal Geol.* **2015**, *144–145*, 98–110. [CrossRef]
8. Ju, J.; Xu, J. Surface stepped subsidence related to top-coal caving longwall mining of extremely thick coal seam under shallow cover. *Int. J. Rock Mech. Min. Sci.* **2015**, *78*, 27–35. [CrossRef]
9. Wang, J.; Yu, B.; Kang, H.; Wang, G.; Mao, D.; Liang, Y.; Jiang, P. Key technologies and equipment for a fully mechanized top-coal caving operation with a large mining height at ultra-thick coal seams. *Int. J. Coal Sci. Technol.* **2015**, *2*, 97–161. [CrossRef]

10. Chen, Y.; Ma, S.; Yu, Y. Stability Control of Underground Roadways Subjected to Stresses Caused by Extraction of a 10-m-Thick Coal Seam: A Case Study. *Rock Mech. Rock Eng.* **2017**, *50*, 2511–2520. [CrossRef]

11. Bai, Q.; Tu, S.; Wang, F.; Zhang, C. Field and numerical investigations of gateroad system failure induced by hard roofs in a longwall top coal caving face. *Int. J. Coal Geol.* **2017**, *173*, 176–199. [CrossRef]

12. Kong, D.; Jiang, W.; Chen, Y.; Song, Z.; Ma, Z. Study of roof stability of the end of working face in upward longwall top coal. *Arab. J. Geosci.* **2017**, *10*, 185. [CrossRef]

13. Wang, J.; Yang, S.; Li, Y.; Wei, L.; Liu, H. Caving mechanisms of loose top-coal in longwall top-coal caving mining method. *Int. J. Rock Mech. Min. Sci.* **2014**, *71*, 160–170. [CrossRef]

14. Wang, J.; Zhang, J.; Li, Z. A new research system for caving mechanism analysis and its application to sublevel top-coal caving mining. *Int. J. Rock Mech. Min. Sci.* **2016**, *88*, 273–285. [CrossRef]

15. Wang, L.; Cheng, L.B.; Cheng, Y.; Yin, G.; Xu, C.; Jin, K.; Yang, Q. Characteristics and evolutions of gas dynamic disaster under igneous intrusions and its control technologies. *J. Nat. Gas Sci. Eng.* **2014**, *18*, 164–174. [CrossRef]

16. Lu, C.P.; Liu, Y.; Wang, H.Y.; Liu, P.F. Microseismic signals of double-layer hard and thick igneous strata separation and fracturing. *Int. J. Coal Geol.* **2016**, *160–161*, 28–41. [CrossRef]

17. Xuan, D.; Xu, J.; Zhu, W. Dynamic disaster control under a massive igneous sill by grouting from surface boreholes. *Int. J. Rock Mech. Min. Sci.* **2014**, *71*, 176–187. [CrossRef]

18. Chen, Y.; Watanabe, K.; Kusuda, H.; Kusaka, E.; Mabuchi, M. Crack growth in Westerly granite during a cyclic loading test. *Eng. Geol.* **2011**, *117*, 189–197. [CrossRef]

19. Zhao, T.; Zhang, Z.; Tan, Y.; Shi, C.; Wei, P.; Li, Q. An innovative approach to thin coal seam mining of complex geological conditions by pressure regulation. *Int. J. Rock Mech. Min. Sci.* **2014**, *71*, 249–257. [CrossRef]

20. Qian, M.; Shi, P. *Mining Pressure and Strata Control*; Qian, M.G., Shi, P.W., Eds.; China University of Mining and Technology Press: Xuzhou, China, 1992.

21. Qian, M.; Miao, X.; Xu, J. Theoretical study of key stratum in ground control. *J. China Coal Soc.* **1996**, *21*, 225–230.

22. Song, Z.; Jiang, Y.; Liu, J. Theory and model of practical method of mine pressure control. *Coal Sci. Technol. Mag.* **2017**, *2*, 1–10. (In Chinese)

23. Feng, G.; Wang, X.; Kang, L. Analysis on the mechanism of the face-contacted blocks structure in overlying strata above the longwall face. *J. China Coal Soc.* **2008**, *33*, 33–37. (In Chinese)

24. Verma, A.K.; Deb, D. Longwall face stability index for estimation of chock-shield pressure and face convergence. *Geotech. Geol. Eng.* **2010**, *28*, 431–445. [CrossRef]

25. Verma, A.K.; Deb, D. Effect of lithological variations of mine roof on chock shield support using numerical modeling technique. *J. Sci. Ind. Res.* **2006**, *65*, 702–712.

26. Guo, W.; Wang, H.; Dong, G.; Li, L. A case study of effective support working resistance and roof support technology in thick seam fully-mechanized face mining with hard roof conditions. *Sustainability* **2017**, *9*, 935. [CrossRef]

27. Ju, J.; Xu, J. Structural characteristics of key strata and strata behaviour of a fully mechanized longwall face with 7.0 m height chocks. *Int. J. Rock Mech. Min. Sci.* **2013**, *58*, 46–54.

28. Cheng, Y.; Jiang, F.; Pang, J. Research on lateral strata pressure characteristic in goaf of top coal caving in extra thick coal seam and its application. *J. China Coal Soc.* **2012**, *37*, 1088–1093. (In Chinese)

29. Wen, Z.; Zhao, X.; Yin, L.; Xia, H. Study on Mechanical Model and Reasonable Working-Condition Parameters in Mining Stope with Large Mining Height. *J. Min. Saf. Eng.* **2010**, *27*, 255–258. (In Chinese)

30. Yu, L.; Yan, S.; Liu, Q. Determination of support working resistance of top coal caving in extra thick coal seam. *J. China Coal Soc.* **2012**, *37*, 737–2742. (In Chinese)

31. Ning, J.; Wang, J.; Jiang, L.; Jiang, N.; Liu, X.; Jiang, J. Fracture analysis of double-layer hard and thick roof and the controlling effect on strata behavior: A case study. *Eng. Fail. Anal.* **2017**, *81*, 117–134. [CrossRef]

32. Huang, B.; Wang, Y.; Cao, S. Cavability control by hydraulic fracturing for top coal caving in hard thick coal seams. *Int. J. Rock Mech. Min. Sci.* **2015**, *74*, 45–57. [CrossRef]

33. Wang, P.; Jiang, J.; Zhang, P.; Wu, Q. Breaking process and mining stress evolution characteristics of a high-position hard and thick stratum. *Int. J. Min. Sci. Technol.* **2016**, *26*, 563–569. [CrossRef]

34. Huang, P.; Ju, F.; Jessu, K.; Xiao, M.; Guo, S. Optimization and Practice of Support Working Resistance in Fully-Mechanized Top Coal Caving in Shallow Thick Seam. *Energies* **2017**, *10*, 1406. [CrossRef]

35. Li, M.; Zhou, N.; Zhang, J.; Liu, Z. Numerical Modelling of Mechanical Behavior of Coal Mining Hard Roofs in Different Backfill Ratios: A Case Study. *Energies* **2017**, *10*, 1–18.

36. Zhou, N.; Zhang, J.; Hao, Y.; Li, M. Deformation Behavior of Hard Roofs in Solid Backfill Coal Mining Using Physical Models. *Energies* **2017**, *10*, 557. [CrossRef]

37. Xie, G.X.; Chang, J.C.; Yang, K. Investigations into stress shell characteristics of surrounding rock in fully mechanized top-coal caving face. *Int. J. Rock Mech. Min. Sci.* **2009**, *46*, 172–181. [CrossRef]

38. Liu, Y.; Zhou, F.; Liu, L.; Liu, C.; Hu, S. An experimental and numerical investigation on the deformation of overlying coal seams above double-seam extraction for controlling coal mine methane emissions. *Int. J. Coal Geol.* **2011**, *87*, 139–149.

39. Lin, Y. *Experimental Rock Mechanics—Simulation Study*; Beijing Industry Press: Beijing, China, 1984.

40. Zhou, A. *Research on Geology of Datong Late Paleozoic Coal-Bearing Basin*; China Coal Industry Press: Beijing, China, 2010.

41. Guo, J.; Feng, G.; Guo, Y.; Qi, T.; Zhang, Y.; Ren, A.; Kang, L.; Guo, G. Mechanical property variation under dynamic uniaxial compression and mechanism of lamprophyre in saturated state. *J. China Coal Soc.* **2015**, *40*, 323–330. (In Chinese)

42. Li, Z.; Guo, J.; Feng, J. Experiment Research on Mechanical Property of Lamprophyre in Nature and Saturated Conditions. *Chin. J. Undergr. Sp. Eng.* **2014**, *10*, 1039–1046. (In Chinese)

43. Deere, D. *The Rock Quality Designation (RQD) Index in Practice*; ASTM International: West Conshohocken, PA, USA, 1988.

44. Liu, Z.; Dang, W. Rock quality classification and stability evaluation of undersea deposit based on M-IRMR. *Tunn. Undergr. Sp. Technol.* **2014**, *40*, 95–101. [CrossRef]

45. Yan, R.; Shen, Y. Correlation of Revised BQ System in China and the International Rock Mass Classification Systems. *J. Civ. Eng. Res.* **2015**, *5*, 33–38.

46. Yan, T.; Wu, X.; Wu, L. Correlation Study on Surrounding Rockmass Classification for Underground Cavern and Its Application. *Chin. J. Undergr. Sp. Eng.* **2009**, *5*, 1103–1109. (In Chinese)

47. Xu, J.; Qian, M. Method to Disting ui sh Key St rata in Ov erburden. *J. China Univ. Min. Technol.* **2000**, *29*, 463–467. (In Chinese)

48. China Coal Industry Press. *State Administration of Work Safety Coal Mine Safety Regulation*; China Coal Industry Press: Beijing, China, 2016.

49. Qian, M.; Miao, X.; He, F. Analysis of key block in the structure of voussoir beam in longwall mining. *J. China Coal Soc.* **1994**, *19*, 557–563. (In Chinese)